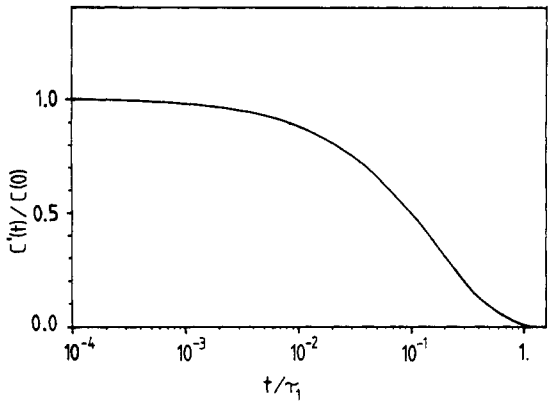

Figure 1. Reduced values $C'(t)/C(0)$ of the q^4 term as a function of reduced time t/τ_1, where τ_1 is the terminal nondraining Zimm viscoelastic relaxation time.

problem that will be discussed elsewhere.

Acknowledgment. M.S. thanks the Alexander von Humboldt Stiftung for a Feodor Lynen Research Fellowship, during the period of which this work was performed. We also thank the National Science Foundation for support of this research under Grant No. DMR 79-13227, Division of Materials Research, Polymers Program, and Grant No. CHE-8000910. The stimulating interest of Professor Walther Burchard is much appreciated.

References and Notes

(1) Berne, B.; Pecora, R. "Dynamic Light Scattering"; Wiley: New York, 1976.
(2) DeGiorgio, V.; Corti, M.; Giglio, M. "Light Scattering in Liquids and Macromolecular Solutions"; Plenum Press: New York, 1980.
(3) Akcasu, A. Z.; Gurol, H. *J. Polym. Sci., Polym. Phys. Ed.* **1976**, *14*, 1.
(4) Akcasu, A. Z.; Benmouna, M.; Han, C. C. *Polymer* **1980**, *21*, 866.
(5) Akcasu, A. Z.; Higgins, J. S. *J. Polym. Sci., Polym. Phys. Ed.* **1977**, *15*, 1745.
(6) Benmouna, M.; Akcasu, A. Z. *Macromolecules* **1980**, *13*, 409.
(7) Burchard, W. *Macromolecules* **1978**, *11*, 455.
(8) Schmidt, M.; Burchard, W. *Macromolecules* **1978**, *11*, 460.
(9) Burchard, W.; Schmidt, M.; Stockmayer, W. H. *Macromolecules* **1980**, *13*, 580.
(10) Burchard, W.; Schmidt, M.; Stockmayer, W. H. *Macromolecules* **1980**, *13*, 1265.
(11) Schmidt, M.; Burchard, W. *Polymer* **1980**, *21*, 745.
(12) Stockmayer, W. H.; Burchard, W. *J. Chem. Phys.* **1979**, *70*, 3138.
(13) Stockmayer, W. H.; Schmidt, M. *Pure Appl. Chem.* **1982**, *54*, 407.
(14) Tanaka, G.; Stockmayer, W. H. *Proc. Natl. Acad. Sci. U.S.A.*, in press.
(15) Kirkwood, J. G.; Riseman, J. *J. Chem. Phys.* **1948**, *16*, 565.
(16) Yamakawa, H. "Modern Theory of Polymer Solutions"; Harper and Row: New York, 1971.
(17) Kirkwood, J. G. *J. Polym. Sci.* **1954**, *12*, 1.
(18) Harvey, S. C. *J. Chem. Phys.* **1979**, *71*, 4221.
(19) Fixman, M. *Macromolecules* **1981**, *14*, 1710.
(20) Akcasu, A. Z. *Macromolecules* **1982**, *15*, 1321.
(21) Zimm, B. H. *J. Chem. Phys.* **1956**, *24*, 269.
(22) Dubois-Violette, E.; de Gennes, P.-G. *Physics (Long Island City, N.Y.)* **1967**, *3*, 181.
(23) Schurr, J. M. *J. Chem. Phys.* **1981**, *74*, 1428.
(24) Schmidt, M.; Burchard, W. *Macromolecules* **1981**, *14*, 210.
(25) Ter Meer, H.-U.; Burchard, W.; Wunderlich, W. *Colloid Polym. Sci.* **1980**, *258*, 675.
(26) Zimm, B. H. *Macromolecules* **1980**, *13*, 593.
(27) Pecora, R. *J. Chem. Phys.* **1965**, *43*, 1562.
(28) Zimm, B. H.; Roe, G. M.; Epstein, L. F. *J. Chem. Phys.* **1956**, *24*, 279.
(29) Hearst, J. E. *J. Chem. Phys.* **1962**, *37*, 2547.
(30) Stockmayer, W. H. *J. Phys. (Orsay, Fr.)* **1971**, *C5a*, 255.
(31) Bantle, S.; Schmidt, M.; Burchard, W. *Macromolecules* **1982**, *15*, 1604.

Neutron Quasi-Elastic Scattering by Small-Ring Polymers

Jean-Louis Viovy* and Lucien Monnerie

Laboratoire de Physicochimie Structurale et Macromolêculaire, ESPCI, 75231 Paris Cedex 05, France. *Received July 21, 1981*

ABSTRACT: The quasi-elastic incoherent neutron scattering spectrum for ring polymers in the Rouse regime is computed on the basis of a next-neighbor diffusion model. The evolution equation involves an orientation correlation due to fixed bond angles and a particular distance scaling due to next-neighbor bond correlations. In the case of a small-ring polymer, an exact mode analysis is possible and gives rise to an expression for the quasi-elastic line shape appropriate for any model leading to an evolution equation of the diffusion type (in one dimension). The translational autocorrelation function, the half-width at half-height, and the quasi-elastic line shape for different ring sizes and static correlations as predicted by the freely jointed chain and the next-neighbor diffusion models are presented and discussed.

Introduction

Quasi-elastic scattering by polymers in the melt and in solution has interested theoreticians for a long time. In 1967, de Gennes[1] predicted for an infinite Rouse chain a q^4 dependence of both incoherent and coherent spectra half-width, $\Delta\omega(q)$, in the low-q, long-time limit. This work was extended[2] by Dubois-Violette and de Gennes to include hydrodynamic interactions, thus predicting a q^3 dependence of $\Delta\omega(q)$. These predictions have been successfully checked by experiments.[3,4] Moreover, the validity of these unusual q dependences seemed to extend to unexpectedly high q values: $q\sigma \sim 1$, where σ is the bond length of the chain. At low q values the de Gennes regime is limited by the overall diffusion of the molecule (which has a finite size) and there should appear a crossover to a classical q^2 dependence. At high q values, neutron scattering is only sensitive to local motions, and the following question arises: Does the spectrum behave as predicted by a local conformation jump model or not (see, for example, ref 5 and 6)?

In a series of papers[7-9] Akcasu et al. applied the Zwanzig–Mori formalism to polymer solutions in order to investigate the crossover between these different regimes. These authors used the bead–spring and freely jointed

0024-9297/82/2215-1611$01.25/0

chain models and derived expressions for $\Delta\omega(q)$, which depends on the chain size, and hydrodynamic interactions. In the latest paper of the series they computed normalized shape functions for the coherent quasi-elastic spectrum in different q ranges, including the transition regions ($qR_g \simeq 1$ and $q\sigma \simeq 1$, where R_g and σ are the radius of gyration of the chain and the bond length, respectively). As pointed out by the authors the results of these computations become qualitative when $q\sigma$ becomes comparable to or larger than unity. Moreover, the results probably cannot be applied to small polymers: small polymers cannot be considered as Gaussian or expanded coils, so that their translation and rotation diffusion coefficients can no longer be simply related to the Rouse time and included in the computation of spectra with the same assumptions as above.

Nevertheless, the incoherent quasi-elastic spectra of some pure flexible-ring molecules such as ring polyethers seem to present some polymer-like features.[22] It is thus tempting to use these compounds to study polymer dynamics in the melt at the scale of a few bonds.

We report here the application to neutron scattering of a diffusion model first proposed by Monnerie et al.[10,11] and successfully applied to a variety of experimental techniques. This model is still very naive. Nevertheless, it may represent a step forward in the understanding of local constraints and of their effects on polymer dynamics.

The model is briefly described and applied to the case of ring polymers in part I. We focus on the $q\sigma \lesssim 1$ region and restrict ourselves to incoherent scattering by small-ring polymers. Under these conditions, it is possible to perform an exact mode analysis and to separate translation from conformational changes as will be shown in part II.

Part III is devoted to numerical computation and a discussion of the results.

I. Model

Different authors have proposed replacing the freely jointed chain (FJC) model by a more realistic one involving conformational transitions of an sp^3 skeleton. These conformational transitions must be correlated in order to compensate and avoid wide swinging motions of the tails. Such motions involving small parts of a chain and leaving the rest unchanged are the so-called Schatzki,[14] Pechold,[15] three-bond, and four-bond[10] motions. Monte Carlo simulations[16] showed that the simplest ones were by far the most probable and supported the use of the three-bond jump as the elementary motion for a dynamic model of sp^3-atom chains.

In a model proposed by Valeur et al.[11] (henceforth referred to as the VJGM model), an sp^3 chain performs three-bond jumps on a tetrahedral lattice imposed by fixed valence angles. Such a three-bond jump would imply an activation energy corresponding to twice that of a rotation potential barrier, in contradiction with experiments.[17,18] More recent studies on reaction kinetics[13] and molecular dynamics[12] seem to rule out the three-bond motion: the reaction coordinate is localized on an atom but the single-bond conformational transition is "helped" by torsion deformations of the neighboring bonds. The striking points in the conclusions of ref 12 are the following: (i) conformational jumps happen mainly for trans configurations, i.e., when series of next neighbors are parallel to each other (in correlation language, this means that for atoms involved in a motion the static cross-correlation function is a function rather slowly decaying in space); (ii) jumps involving next neighbors are strongly correlated.

We propose to use these two features in the construction of the diffusion equation for polymer chains, without relating them to a particular molecular motion. This model will be referred to as the next-neighbor diffusion (NND) model.

Calling $\mathbf{u}_n$ the nth bond of an N-atom ring polymer, we can write the diffusion equation with next-neighbor interaction as

$$\partial\mathbf{u}_n/\partial t = W(\mathbf{u}_{n-2} - 2\mathbf{u}_n + \mathbf{u}_{n+2}) \qquad (n \neq 1, 2, N-1, N) \quad (1)$$

where W is the elementary frequency of the orientational change.

Since we are interested in pure polymers at a short length scale, it is not necessary to take into account long-range hydrodynamic interactions, and calculations can be performed in the Rouse regime. For the sake of simplicity we shall develop in the following only the case for N even.

Calling $\mathbf{U}$ the $3 \times N$ vector of the $\mathbf{u}_n$, we can express eq 1 and 2 in matrix form as follows:

$$\partial\mathbf{U}(t)/\partial t = -W\mathbf{K}\mathbf{U}(t) \quad (2)$$

where

$$\mathrm{K} = \begin{bmatrix} 1 & 0 & -1 & 0 & & & & & 0 & -1 & 0 \\ 0 & 1 & 0 & -1 & 0 & & & & 0 & 0 & -1 \\ -1 & 0 & 2 & 0 & -1 & & & & 0 & 0 & 0 \\ 0 & -1 & 0 & 2 & & & & & & & \\ & 0 & -1 & & & & & & & & \\ & & & & & & & -1 & 0 & & \\ & & & & & & 2 & 0 & -1 & 0 & \\ 0 & & & & & -1 & 0 & 2 & 0 & -1 & \\ -1 & 0 & & & & 0 & -1 & 0 & 1 & 0 & \\ 0 & -1 & 0 & & & & 0 & -1 & 0 & 1 & \end{bmatrix} \quad (3)$$

Decomposing into two sets of $M = N/2$ vectors, we separate $\mathbf{K}$ into two independent circulant matrices of order M:

$$\mathrm{K}' = \begin{bmatrix} 1 & -1 & 0 & & & & & 0 & -1 \\ -1 & 2 & -1 & 0 & & & & & 0 \\ 0 & -1 & 2 & & & & & & \\ & 0 & & & & & & & \\ & & & & & & 0 & & \\ & & & & & 2 & -1 & 0 & \\ & & & & 0 & -1 & 2 & -1 & \\ 0 & & & & & 0 & -1 & 1 & \\ -1 & 0 & & & & & & & \end{bmatrix} \quad (4)$$

The mode analysis of $\mathbf{K}'$ is classical and leads to the solution

$$c_j(t) = M^{-1}\sum_{l=1}^{M}\sum_{p=1}^{M}\cos\frac{2\pi p(j-l)}{M}e^{-Wt\lambda_p}c_l(0) \quad (5)$$

with

$$\lambda_p = 4\sin^2\left(\frac{p\pi}{M}\right) \quad (6)$$

The slowly decaying static cross correlation (feature i) can be introduced into the model to take into account the existence of privileged bond angles:

$$\langle\mathbf{u}_n(0)\mathbf{u}_m(0)\rangle = \varphi_0(n,m) \quad (7)$$

This leads to a next-neighbor diffusion equation with correlation (NNDC).

At present, the shape of φ_0 cannot be evaluated from molecular dynamics, and we approximate it by an exponential:

$$\varphi_0(i,j) = \exp(-\gamma|i - j|) \tag{8}$$

γ measures the correlation and can be obtained approximately by conformation calculations (for example, γ is 2.19 for an equally weighted chain and approximately 0.7 for polyethylene).

It can be seen that the VJGM model also leads to eq 1–7: this can explain why it has been so successful in the interpretation of fluorescence, dielectric, and NMR data, in spite of its unrealistic molecular basis.

Taking φ_0 as a δ function leads to the same correlation function as would be obtained from a freely jointed chain model (FJC), except for a factor of 2 in the limit of summation. This is due to the fact that the FJC model involves first-neighbor interactions instead of next-neighbor ones. We shall use this property in the following to perform the exact mode analysis in the FJC model as well as in the NNDC model. The FJC model will be a useful basis for discussing the effect of the correlations introduced in the NNDC model.

II. Incoherent Quasi-Elastic Neutron Scattering Spectrum

So far as only intrachain interactions are concerned, coherent scattering generally gives no more information than incoherent scattering. Therefore we restrict ourselves to incoherent scattering, which involves simpler correlation functions.

The incoherent spectrum is given by

$$S(q,\omega) = \frac{1}{2\pi}\int \mathrm{d}t\, I(q,t) \exp(-i\omega t) \tag{9}$$

$$I(q,t) = \langle \exp(-i\mathbf{q}\cdot\mathbf{R}_n(0)) \exp(i\mathbf{q}\cdot\mathbf{R}_n(t)) \rangle \tag{10}$$

where $\mathbf{R}_n$ is the position of the nth scattering center. We consider hydrogen atoms only and suppose them centered on the carbon atom to which they are bonded. This is, of course, a major limitation of the model and should be taken into account when real polymers are involved; we believe this approximation to be acceptable for polyethylene or aliphatic polyethers but certainly not for chains with pendant groups. The other main limitation is the so-called Gaussian approximation: in order to treat the model to the end, we must suppose, as other authors,

$$I(q,t) \simeq \exp(-\tfrac{1}{6}q^2 A(t)) \tag{11}$$

where

$$A(t) = \langle |\mathbf{R}_n(0) - \mathbf{R}_n(t)|^2 \rangle \tag{12}$$

Due to the q range involved in our model, we expect it to apply mainly to experiments performed on back-scattering or time-of-flight devices, i.e., in the frequency domain. Therefore the dynamic structure factor $S(q,\omega)$ will be our main concern. As pointed out above, translation and overall rotation times cannot be simply related to the elementary frequency W. Thus, instead of giving them an arbitrary value or covering their whole available range, we present out results in terms of $S^{\mathrm{Q}}(q,\omega)$. The "quasi-elastic" part $S^{\mathrm{Q}}(q,\omega)$ is the wide line in $S(q,\omega)$ deconvoluted from the narrow one. We do not believe this separation of $S(q,\omega)$ to be a serious experimental restriction since experimentalists are generally obliged to perform it anyway due to the finite frequency window of neutron scattering spectrometers. Moreover, overall translation and rotation coefficients can sometimes be measured precisely by other techniques such as NMR and pulsed gradient spin-echo NMR, thus improving deconvolution and separation of the two components in $S(q,\omega)$. From a theoretical point of view, this separation implies a weak coupling between internal motions and overall translation–rotation. Translation can be rigorously separated in the model by use of a molecular frame related to the center of mass of the molecule. But, obviously, conformational changes, as defined in our model (or the freely jointed chain), can lead to any orientation in space of a given conformational state. So the separation between internal motions and overall tumbling is to some extent arbitrary. This is a very general problem (it concerns, as a matter of fact, any flexible molecule) and a hard one. It has been solved only for very simple molecules (see, for example, ref 19 and 20). Therefore we believe that an arbitrary separation between rotation and conformational changes will remain as a necessary ingredient of any dynamical model involving molecules with a high number of degrees of freedom. Of course, in the case of polymers, this is troublesome only for short chains, $N \lesssim 100$. Fortunately, NMR measurements on 1,4,7,10,13,16-hexaoxacyclooctadecane (18-crown-6)[21] indicate that for the kind of molecules we deal with, rotation in the pure liquid state is very slow compared to internal motions,[22] thus justifying the separation hypothesis.

We separate $A(t)$ into a slowly decaying function $A^0(t)$ related to overall motions and a fast component $A^{\mathrm{Q}}(t)$ related to internal motions:

$$A(t) = A^0(t) + A^{\mathrm{Q}}(t) \tag{13}$$

$$A^{\mathrm{Q}}(t) = \langle (\mathbf{r}_n(0) - \mathbf{r}_n(t))^2 \rangle \tag{14}$$

where $\mathbf{r}_n(t)$ is the position of the nth atom in the molecular frame. Then

$$I(q,t) = I^0(q,t)I'(q,t) \tag{15}$$

where

$$I'(q,t) = \exp(-\tfrac{1}{6}q^2 A^{\mathrm{Q}}(t)) = I^{\mathrm{Q}}(q,t)I^{\mathrm{E}}(q) \tag{16}$$

and

$$I^{\mathrm{Q}}(q,t) = \exp(-\tfrac{1}{6}q^2 A^{\mathrm{Q}}(\infty))[\exp(-\tfrac{1}{6}q^2(A^{\mathrm{Q}}(t) - A^{\mathrm{Q}}(\infty))) - 1] \tag{17}$$

$$I^{\mathrm{E}}(q) = \exp(-\tfrac{1}{6}q^2 A^{\mathrm{Q}}(\infty)) \tag{18}$$

$I^{\mathrm{E}}(q)$ is the elastic incoherent structure factor, and the Fourier transform of $I^{\mathrm{Q}}(q,t)$ is the quasi-elastic line shape $S^{\mathrm{Q}}(q,\omega)$.

$\mathbf{r}_n(t)$ can be related to the bond vectors $\mathbf{u}_i(t)$ by

$$\mathbf{r}_n = \mathbf{r}_i - \sum_{j=i+1}^{n} \mathbf{u}_j \tag{19}$$

In particular, for whatever i, $1 \le i < N$

$$\mathbf{r}_N = \mathbf{r}_i + \sum_{j=i+1}^{N} \mathbf{u}_j \tag{20}$$

and, summing up on i

$$N\mathbf{r}_N = \mathbf{r}_N + \sum_{i=1}^{N-1} \mathbf{r}_i + \sum_{i=1}^{N-1} \sum_{j=i+1}^{N} \mathbf{u}_j \tag{21}$$

which leads for the atom origin of the numbering (which is arbitrary)

$$\mathbf{r}_N = N^{-1} \sum_{i=1}^{N-1} \sum_{j=i+1}^{N} \mathbf{u}_j \tag{22}$$

Then the expression for $A^{\mathrm{Q}}(t)$ in the freely jointed chain model is

$$A_1^Q(t) = \frac{2\sigma^2}{N^2} \sum_{i=1}^{N-1} \sum_{j=i+1}^{N} \sum_{k=1}^{N-1} \sum_{l=k+1}^{N} (c_j^l(0) - c_j^l(t)) \quad (23)$$

where

$$\sigma^2 c_j^l(t) = \langle \mathbf{u}_j(0)\mathbf{u}_l(t) \rangle \quad (24)$$

i.e., from (5), (14), and (23)

$$c_j^l(t) = N^{-1} \sum_{p=1}^{N} \cos\left(\frac{2\pi p(l-j)}{N}\right) \exp(-Wt\lambda_p) \quad (25)$$

In the NNDC model, separation between odd–odd, odd–even, and even–even terms leads to the following expression for $A^Q(t)$:

$$A_2^Q(t) = \frac{4\sigma^2}{M^2} \sum_{i=1}^{M-1} \sum_{j=i+1}^{M} \sum_{k=1}^{M-1} \sum_{l=k+1}^{M} (c'^l_j(0) - c'^l_j(t)) \quad (26)$$

where, after (5), (7), and (8)

$$c'^l_j(t) = M^{-1} \sum_{i=a}^{b} \sum_{p=1}^{M} \cos\left(\frac{2\pi l(j-l)}{M}\right) \exp(-Wt\lambda_p - \gamma|i-l|) \quad (27)$$

$$a = i - \frac{M}{2} \quad (M \text{ even}) \quad \text{or} \quad i - \left(\frac{M-1}{2}\right) \quad (M \text{ odd})$$

$$b = i + \frac{M}{2} - 1 \quad (M \text{ even}) \quad \text{or} \quad i + \left(\frac{M-1}{2}\right) \quad (M \text{ odd})$$

Equations 14 and 23–27 allow us to compute the spectra $I^Q(q,t)$ and $S^Q(q,\omega)$ for any values of N, t, q, and γ.

III. Results

III.1. Mean-Square Displacement. We first compute the mean-square displacement (with regard to the center of mass) for the freely jointed chain, $A_1^Q(t)$, for different values of N. As expected from scaling considerations,[1] $A_1^Q(t)$ tends to be proportional to N for N high enough. Results are compared in Figure 1 by means of the reduced variables $(tW/N^2, A^Q(t)/N\sigma^2)$. When N increases, the curves tend to a limit. The model is thus compatible with scaling laws: $A_1^Q(t,N)$ has a constant shape for $N \gtrsim 20$ to the precision of our computations. As expected, the initial slope increases when N increases (for $N \to \infty$, $[\partial(A^Q(t)/N\sigma^2)/\partial t]_{t=0}$ must tend to ∞[1]).

Comparison with the NNDC model is made in Figure 2 ($N = 18$). The FJC curve (dashed) is very similar to the NNDC curve, with $\gamma = \infty$ (the difference arises from the alternate coupling in our model: as can be seen from eq 15–18, $A_2^Q(t,N)$ is identical with $A_1^Q(t,N/2)$, except for a scaling factor. When γ decreases (increasing orientation correlation), the mean-square displacement at infinite time increases to a limiting value (here for $\gamma \simeq 1$). When γ decreases further, the correlation length becomes comparable to the cycle size. An overall rigidity follows, which reduces mobility, as can be seen on curves $\gamma = 0.7$ and $\gamma = 0.2$ (Figure 2).

As a consequence of the Gaussian hypothesis, the models lead to a Gaussian EISF ($I^E(q)$), directly related to $A^Q(\infty)$: the half-width at half-height $(q\sigma)^H$ is given by

$$0.5 = \exp\left(-\frac{1}{6\sigma^2}((q\sigma)^H)^2 A^Q(\infty)\right) \quad (28)$$

and numerical values are presented in Table I for different values of N and γ. It is an important parameter for experiments: The lower $I^E(q)$, the better the precision on the quasi-elastic line.

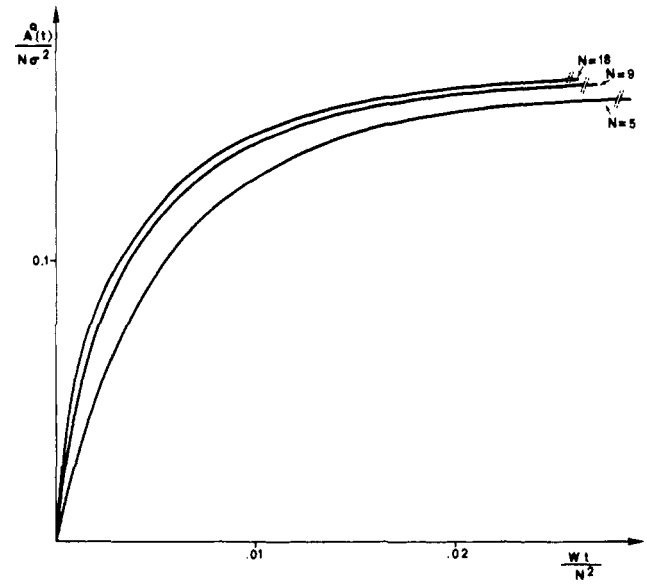

Figure 1. $A_1^Q(t)$ for the FJC model (scaled).

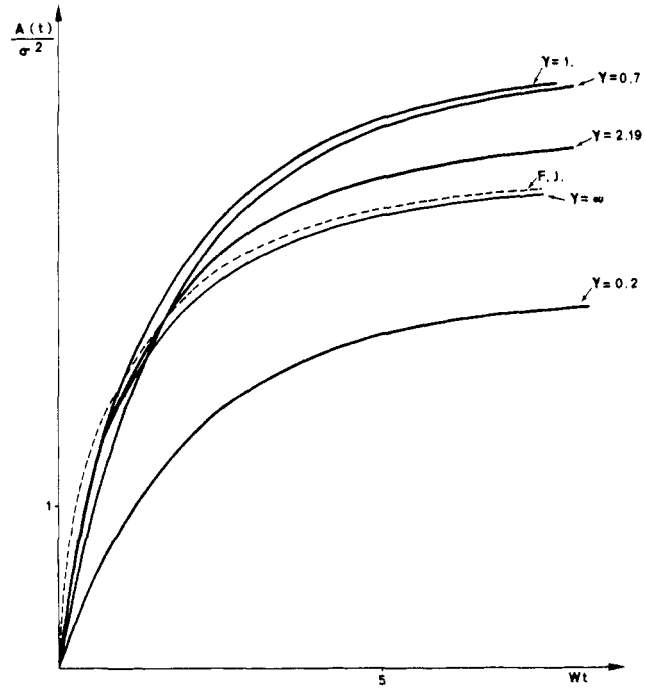

Figure 2. $A_2^Q(t)$ for the NNDC model ($N = 18$) and different values of γ. The FJC curve, $N = 18$, is given for comparison (dashed line).

Table I
Half-Width at Half-Height $(q\sigma)^H$ of the Elastic Incoherent Structure Factor $I^E(q)$

FJC model		NNDC model, $N = 18$	
N	$(q\sigma)^H$	γ	$(q\sigma)^H$
5	1.50	∞	0.79
9	1.10	2.19	0.74
18	0.78	1	0.70
		0.7	0.70
		0.2	0.89

III.2. Half-Width at Half-Height of $S(q,\omega)$. The half-width at half-height $\Delta\omega$ of $S(q,\omega)$ has been for a long time the usual experimental access to correlation times, as well as the test data for scaling laws. So we think it is useful to discuss the q dependence of $\Delta\omega$ as obtained from FJC and NNDC models. log $(\Delta\omega)$ is presented as a function of log $(q\sigma)$ in Figure 3. For high enough N values

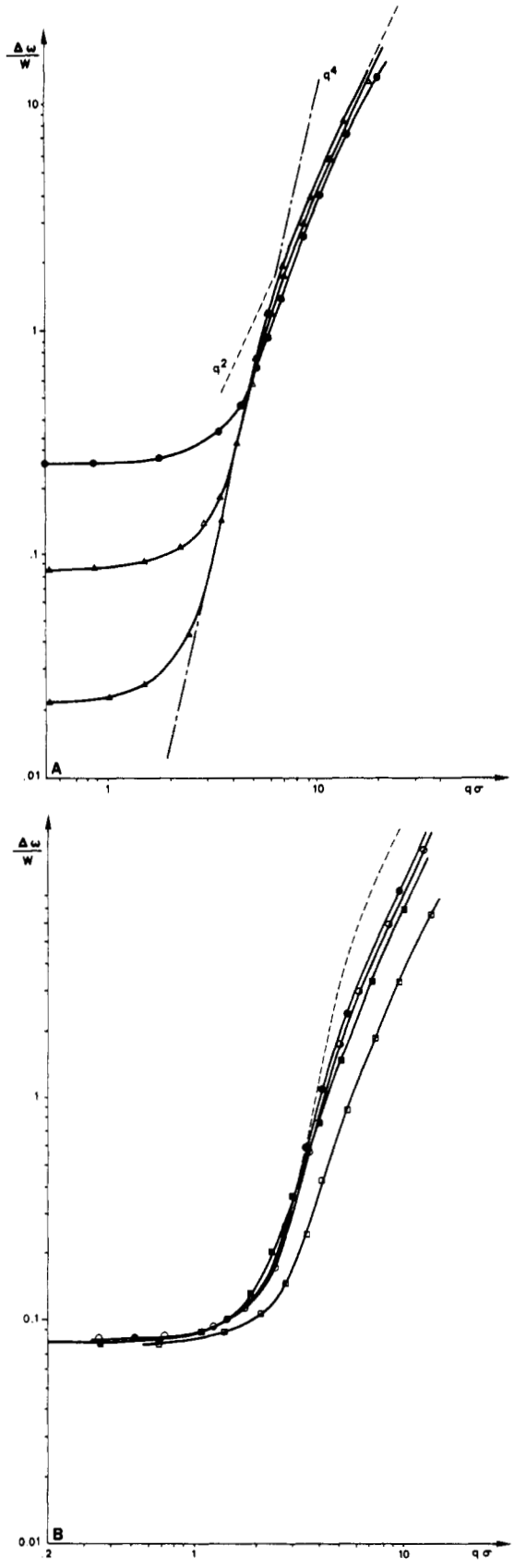

Figure 3. (A) $\Delta\omega = f(q\sigma)$ for the FJC model: (●) $N = 5$; (▲) $N = 9$; (▲) $N = 18$. The lines q^4 (dot–dash) and q^2 (dashed) are given as guides for the eye. (B) $\Delta\omega = f(q\sigma)$ for the NNDC model, $N = 18$: (●) $\gamma = \infty$; (○) $\gamma = 2.29$; (■) $\gamma = 0.7$; (□) $\gamma = 0.2$. The FJC result, $N = 18$, is also shown (dashed line, frequency scaled).

($N \gtrsim 9$), three regimes are obtained.

(i) At high q, $\Delta\omega$ tends to a q^2 behavior for both models; this result can be checked more precisely in Figure 4A,

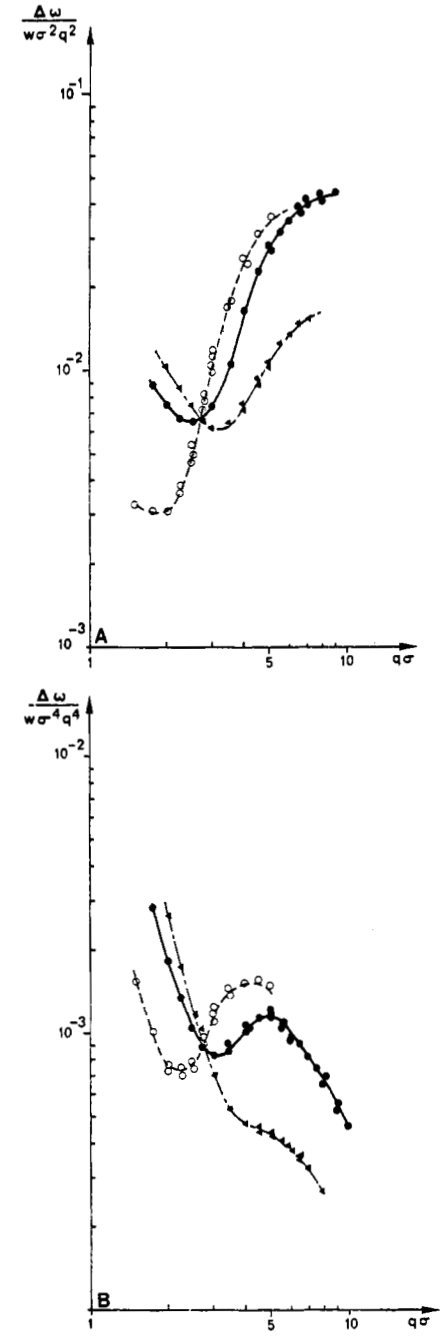

Figure 4. $\Delta\omega/(q\sigma)^x$ for the FJC model, $N = 18$ (full line) and $N = 36$ (dashed line), and for the NNDC model, $N = 30$, $\gamma = 1$ (dash–dot line): (A) $x = 2$; (B) $x = 4$. (The symbols are points computed with various sampling times and time ranges.)

where $\Delta\omega/W(q\sigma)^2$ is plotted as a function of $q\sigma$ (on a log scale). This is a straightforward consequence of the Gaussian hypothesis and as such is rather uninteresting.

(ii) For intermediate q ($2 \lesssim q\sigma \lesssim 5$, depending on N), $\Delta\omega$ has a complex behavior. In Figure 3A (model FJC), log ($\Delta\omega$) seems to follow a q^4 law, as predicted by asymptotic laws, but the plot of log $(\Delta\omega/W(q\sigma)^4)$ as a function of log $(q\sigma)$ (Figure 4B) presents a domain of positive slope, indicating that the exponent of $\Delta\omega = f(q)$ exceeds 4. This effect was carefully checked not to be a truncation effect in the Fourier transform by varying sampling time and time range. It does not seem to be due to the small size of the ring, since it is emphasized where N is increased.

This particular shape disappears when a sufficient correlation is introduced, and a monotonous behavior of $\Delta\omega/q^4$ is recovered (Figure 4B, dash–dot line). This decrease in the slope is a consequence of the lower initial

slope in $A(t)$ (see Figure 2). Unfortunately, computation cost increases very rapidly with N, so that it has been impossible to check if for a fixed value of γ, $\Delta\omega/q^4$ remains monotonous at larger N.

(iii) When $^1/_6q^2A^Q(\infty)$ becomes smaller than 1, diffusion is limited by the polymer size itself. The spectrum is then the superposition of the overall diffusion central line and a wider quasi-elastic line. When q tends to zero, the half-width at half-height of this line tends to a limiting value, which depends on the number of atoms and the jump frequency. Its intensity decreases to zero.

The crossover between regimes (ii) and (iii) reflects the mean displacement at infinite time $A^Q(\infty)$.

In the FJC model the corresponding q value depends only on the chain length, as shown in Figure 3A. For the NNDC model there is an additional effect coming from orientation correlation. Such an effect is reported in Figure 3B, in which the correlation parameter γ is varied at constant chain length. For weak correlations ($0.7 \leq \gamma \leq 2.19$), the $\Delta\omega = f(q)$ curve is scarcely changed, whereas for stronger correlations (lower γ values), it is shifted toward large q.

Different authors[9,13] have already argued against the use of $\Delta\omega$ for precise studies of polymer dynamics. The anomalies observed in the intermediate q range strongly support this point of view. In some cases[23] data treatment can be greatly improved by the cumulant analysis. Unfortunately, this analysis, proposed and developed by Akcasu et al.[9] within a model for coherent scattering based on the eigenfunction expansion method, is irrelevant here: indeed the first cumulant in our model for incoherent scattering follows an uninteresting q^2 law, as can be seen from eq 16. As we impose the size of the smallest moving unit and make in the following no expansion or continuous approximation, the initial slope in $I(q,t)$ reflects only the frequency of the elementary step (in mode language, $\Omega(q)$ reflects only the high-frequency cutoff contained in our starting assumptions).

As a consequence, the present computations should, when possible, be compared with experiment by fitting procedures using the shape of $S(q,\omega)$.

This improved treatment may soon become the usual one in neutron scattering, as suggested by the recent extension of Akcasu's work to numerical computation of shape functions.[24]

III.3. Shape Functions for $S(q,\omega)$. It has long been known that for high polymers the spectrum in the intermediate q^4 domain should be non-Lorentzian.[1] This has been checked recently experimentally, in particular by Richter et al.[4] Figure 5 shows the behavior of $S^Q(q,\omega)$ in the FJC model when $q\sigma$ varies, in comparison to Lorentzian and de Gennes' spectral shapes. At low q values, $S^Q(q,\omega)$ is quasi-Lorentzian. When q increases, the central part narrows and the wing heightens (Figure 5B). The deviation is maximum in the crossover region and is more important than that predicted by de Gennes (dash–dot line). The curve then smoothens again to a Lorentzian.

Figure 6 shows an equivalent behavior in the case of the NNDC model. A striking point is that the orientation correlation tends to lower the non-Lorentzian character of the spectrum. This may explain why rather crude techniques such as simple measure of $\Delta\omega$ are sometimes in surprising agreement with theory (but it should depend a lot on flexibility).

III.4. Shape Function for the Intermediate Quasi-Elastic Scattering Law. From a computational point of view, this section should have preceded section III.3. But since we do not deal with very small scattering angles,

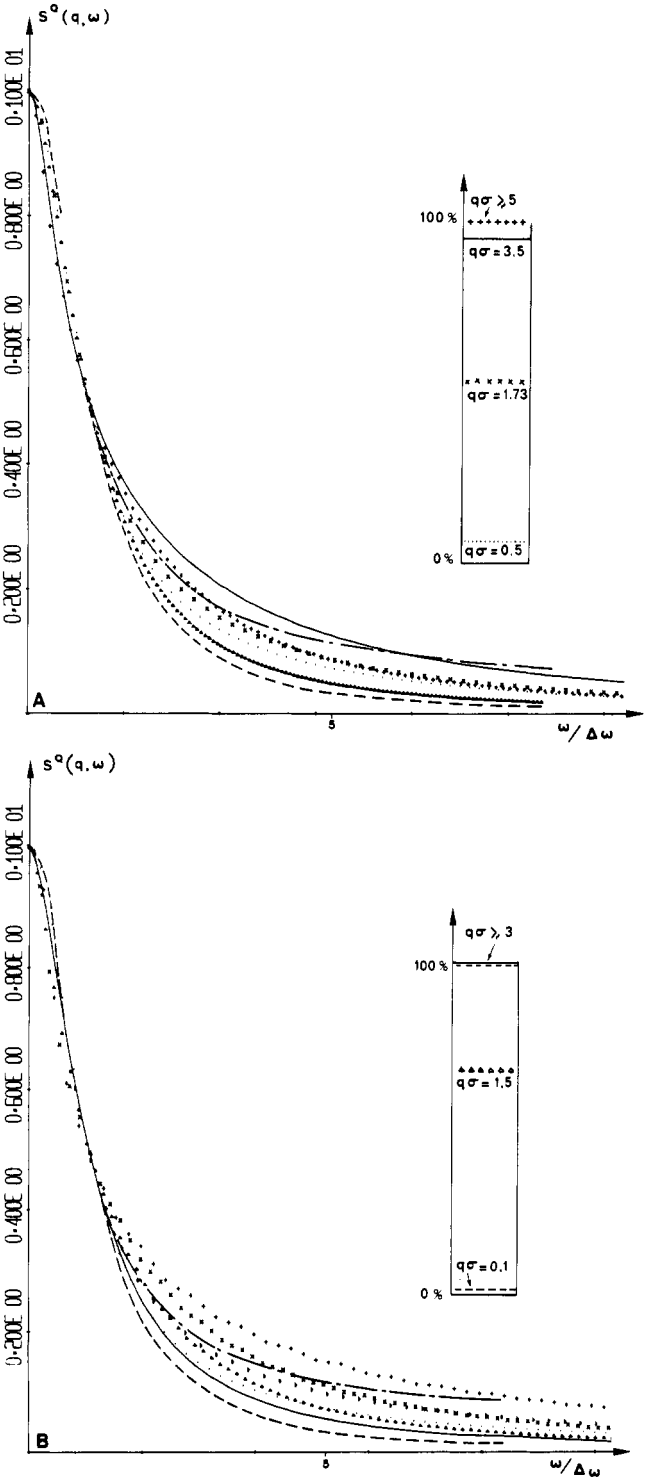

Figure 5. $S^Q(q,\omega)$ for the FJC model (scaled to constant hwhh). The inset shows the contribution of the quasi-elastic line to the total intensity of the spectrum, the dashed line is a Lorentzian, and the dash–dot line a de Gennes function. (A) $N = 9$: $q\sigma$ = 0.5 (●), 1.75 (×), 3.5 (continuous), 5 (+), and 8 (△). (B) $N = 18$: $q\sigma$ = 0.1 (●), 1.5 (▷), 3 (+), 4 (×), 5 (△), and 7 (continuous).

light scattering or neutron spin echo, which measures coherent scattering in the time domain, does not seem to be relevant here.

Nevertheless, the characteristics of a spectrum are often more evident in the time domain, and in Figures 7 and 8 we briefly present on a logarithmic scale a comparison between the two explored models. Notice we represent $I(q,t)$ as the product of two terms:

$$I(q,t) = I^0(q,t)[I^Q(q,t) + I^E(q)] \qquad (29)$$

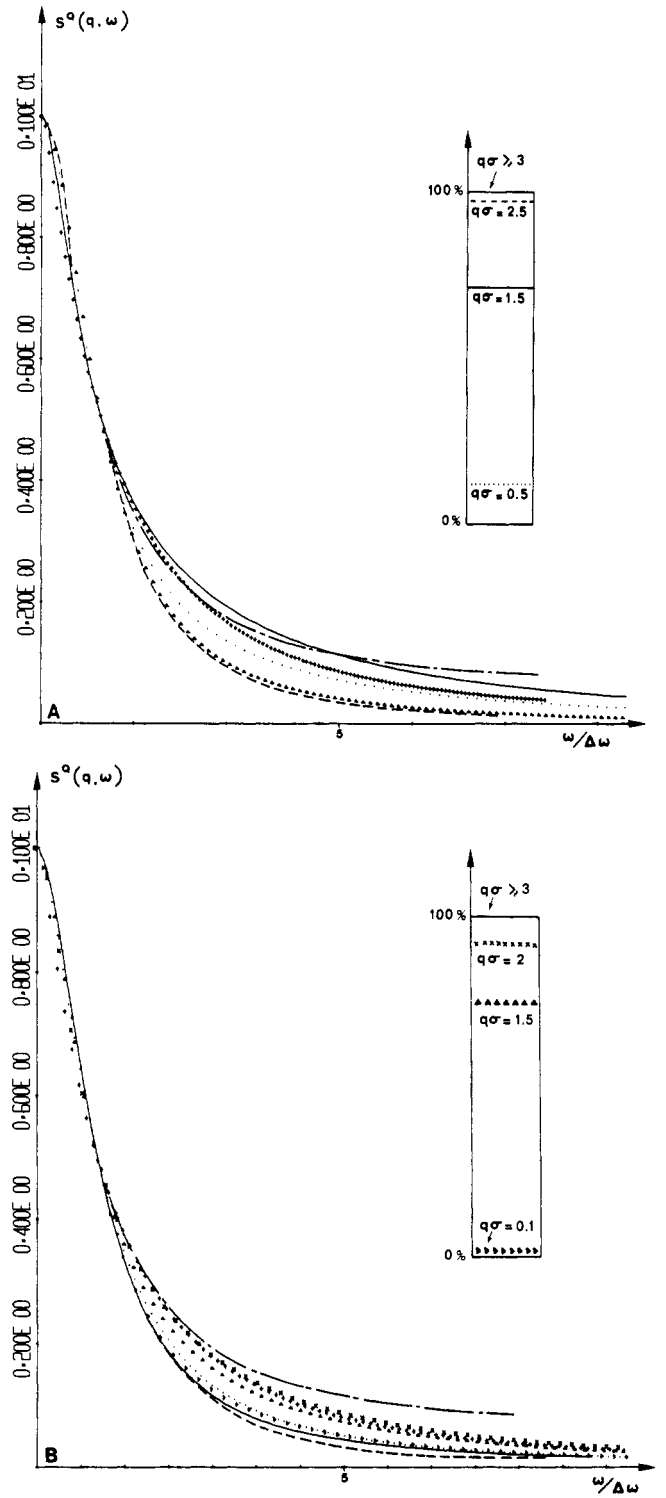

Figure 6. $S^Q(q,\omega)$ for the NNDC model, $N = 18$. (A) $\gamma = 2.19$: $q\sigma = 0.5$ (●), 1.5 (continuous), 2.5 (+), and 7 (△). (B) $\gamma = 0.7$: $q\sigma = 0.1$ (▷), 1.5 (△), 2 (×), 3 (+), 5 (●), and 10 (continuous).

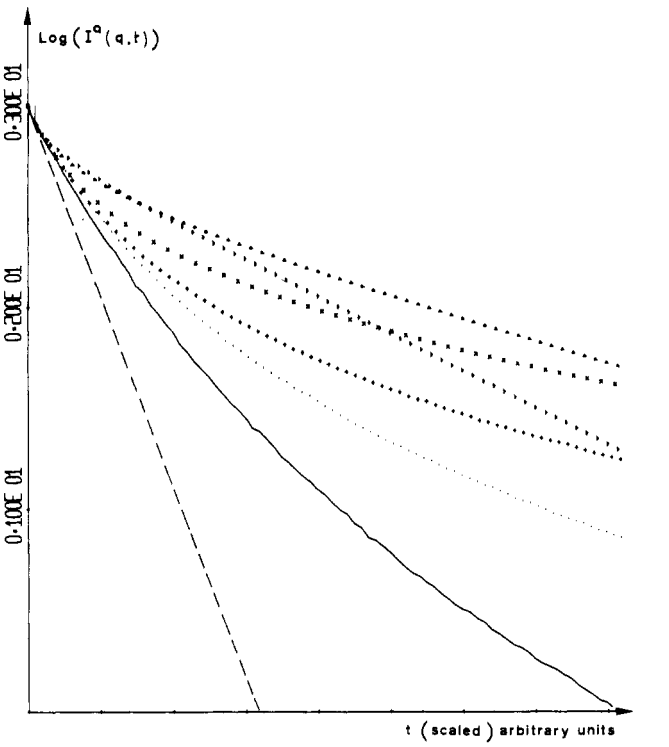

Figure 7. log $(I^Q(q,t))$ as a function of t for the FJC model, $N = 18$, scaled to constant initial slope. The dashed line is a pure exponential. $q\sigma = 0.1$ (▷), 1.5 (△), 3 (×), 4 (+), 5 (●), and 7 (continuous).

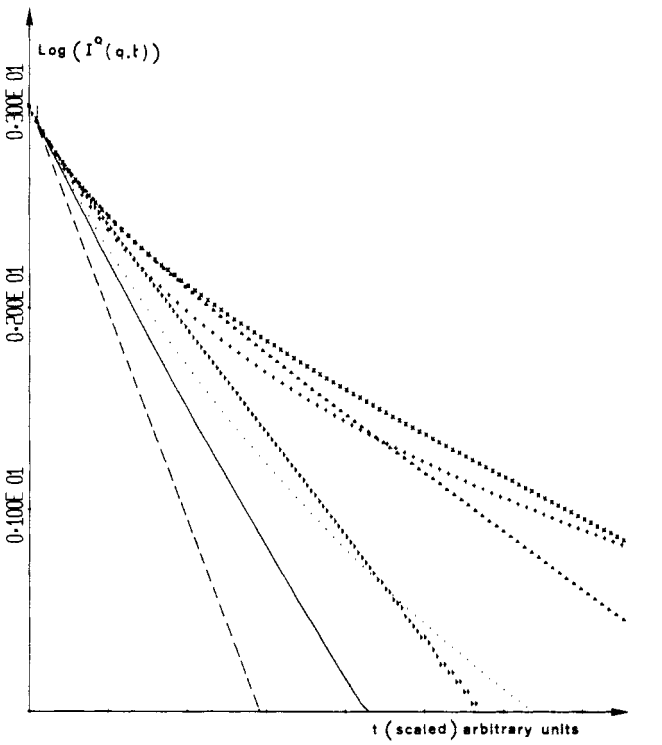

Figure 8. log $(I^Q(q,t))$ as a function of t for the NNDC model, $N = 18$, $\gamma = 0.7$ (scaled to constant initial slope). $q\sigma = 0.1$ (▷), 1.5 (△), 2 (×), 3 (+), 5 (●), and 10 (continuous).

As expected, a deviation from exponential behavior can be observed in both models. It is a maximum around $q_c \simeq 3/\sigma$. Moreover, the nature of the deviation depends strongly on the q domain (Figure 7): for $q < q_c$ there is a steep change in slope at small t and then an almost purely exponential behavior (this is very similar to the behavior of the orientation second-moment autocorrelation function as predicted and observed by Valeur[11]). On the contrary, at high q there is a smooth curvature over the whole time domain, in agreement with the asymptotic behavior.[1] The correlation ($\gamma \neq \infty$) tends to reduce the nonexponential character of the spectrum in any q domain, as apparent in Figures 7 and 8.

IV. Conclusions

In the present paper, we introduced in the diffusion equation for polymer dynamics two features deduced from our knowledge of local conformation and got a next-neighbor diffusion with correlation (NNDC) model, more

realistic than the freely jointed chain model. These two features are first, an orientation correlation factor, related to preferred conformations, and second, a different scaling of bond length, due to next-neighbor correlations. Both seem to be supported by recent molecular dynamics calculations.

We looked for a more precise description of the neutron quasi-elastic spectrum when $q\sigma \simeq l$ by an exact solution of the mode equation. This requires heavier calculation and numerical solutions. Thus we restricted ourselves to small-ring polymers in the Rouse regime and chains of 50 atoms or less.

In the classical freely jointed chain model, the mode analysis leads to line shapes $S(q,\omega)$ that show a q-dependent deviation from Lorentzian shape. This deviation can be larger than that predicted by de Gennes in the asymptotic limit.

The conformational constraints taken into account in the NNDC model strongly reduce this deviation and for small rings hinder the appraisal of a polymer-like behavior.

Since our model takes into account the effective interatomic distances, it must fit experiments over the whole q range of interest by varying only two parameters i.e., the elementary frequency W and the correlation parameter γ. Then comparison with experiment would provide not only a severe check of the model but also an opportunity to measure γ and to get an absolute evaluation of the elementary frequency.

The γ value could be compared with conformational energies or Monte Carlo calculations.[23] This would lead to an interesting insight into the relation between static and dynamic rigidity.

Acknowledgment. We are greatly indebted to Dr. J. C. Lassegues for pointing out to us the striking polymer-like behavior of small-ring molecules and to Dr. J. Dianoux for useful comments on the manuscript.

References and Notes

(1) de Gennes, P.-G. *Physics* **1967**, *3*, 37.
(2) de Gennes, P.-G.; Dubois-Violette, E. *Physics* **1967**, *3*, 181.
(3) Maconnachie, A.; Vasudevan, P.; Allen, G. *Polymer* **1978**, *19*, 33.
(4) Richter, D.; Hayter, J. B.; Mezei, F.; Ewen, B. *Ber. Bunsenges. Phys. Chem.* **1979**, *83*, 380.
(5) Dianoux, A. J.; Volino, F. *Mol. Phys.* **1977**, *34*, 1263.
(6) Barnes, J. D. *J. Chem. Phys.* **1973**, *58*, 5199.
(7) Akcasu, A. Z.; Gurol, H. *J. Polym. Sci., Polym. Phys. Ed.* **1976**, *14*, 1.
(8) Akcasu, A. Z.; Higgins, J. *J. Polym. Sci., Polym. Phys. Ed.* **1977**, *15*, 1745.
(9) Akcasu, A. Z.; Benmouna, M.; Han, C. *Polymer* **1980**, *21*, 866.
(10) Monnerie, L.; Geny, F. *J. Chim. Phys. Phys.-Chim. Biol.* **1969**, *66*, 1961.
(11) Valeur, B.; Jarry, J. P.; Geny, F.; Monnerie, L. *J. Polym. Sci., Polym. Phys. Ed.* **1975**, *13*, 667.
(12) Helfand, E.; Wasserman, Z. R.; Weber, T. A. *Macromolecules* **1980**, *13*, 526.
(13) Skolnick, J.; Helfand, E. *J. Chem. Phys.* **1980**, *72*, 5489.
(14) Schatzki, T. F. *J. Polym. Sci.* **1962**, *57*, 496.
(15) Pechold, W.; Blasenbrey, S.; Woerner, S. *Colloid Polym. Sci.* **1963**, *14*, 189.
(16) Geny, F.; Monnerie, L. *J. Polym. Sci., Polym. Phys. Ed.* **1979**, *17*, 131, 147.
(17) Baysal, B.; Lowry, B. A.; Yu, H.; Stockmayer, W. H. In "Dielectric Properties of Polymers"; Karasz, F. E., Ed.; Plenum Press: New York, 1972.
(18) Morawetz, H. *Macromolecules* **1976**, *9*, 463.
(19) Evans, G. T. *J. Chem. Phys.* **1978**, *69*, 3363.
(20) Wegener, W. A.; Dowben, R. M.; Koester, V. J. *J. Chem. Phys.* **1980**, *73*, 4086.
(21) Richter, H. Thesis, Universität Karlsruhe, 1980.
(22) Lassegues, J. C.; Fouassier, M.; Lemaire, J., unpublished results.
(23) Higgins, J. S.; Nicholson, L. K.; Hayter, J. B. *Polymer* **1981**, *22*, 163.
(24) Han, C. C.; Akcasu, A. Z. *Polymer* **1981**, *22*, 1099.

Stoichiometric Complexation of Human Serum Albumin with Strongly Acidic and Basic Polyelectrolytes

Etsuo Kokufuta,* Hidetoshi Shimizu, and Isei Nakamura

Institute of Applied Biochemistry, The University of Tsukuba, Sakura-mura, Niihari-gun, Ibaraki 305, Japan. *Received April 7, 1982*

ABSTRACT: Colloid titrations of human serum albumin (HSA) with poly(diallyldimethylammonium chloride) (PDDA) and potassium poly(vinyl alcohol sulfate) (KPVS) were carried out at different pHs. The mole numbers of quaternary ammonium groups in PDDA and sulfate groups in KPVS, which are bound to the acidic (carboxyl, mercapto, and phenolic OH) groups and the basic (amino, imidazolyl, and guanidyl) groups in HSA by salt linkages, respectively, were evaluated by the titration data in the pH range where the ionizable groups in HSA are dissociated completely, i.e., pH >12.5 for the acidic groups and pH <2.5 for the basic groups. The results obtained approximately agree with the contents of the acidic and basic groups in HSA, which are calculated on the basis of the amino acid sequence of HSA. Thus it is indicated that the complexation of HSA with PDDA and also with KPVS follows a stoichiometric relationship in the pH ranges above 12.5 and below 2.5, respectively.

Colloid titration is a useful method for obtaining information about the stoichiometry of the salt linkage formation between the ionizable groups in oppositely charged polyions.[1,2] Previously, we applied this titration technique to study the complexation of human carboxyhemoglobin (Hb) with strongly acidic and basic polyelectrolytes and reported that three kinds of basic groups in Hb stoichiometrically form salt linkages with potassium poly(vinyl alcohol sulfate) (KPVS).[3] Moreover, the acidic groups remaining in the Hb–KPVS complex are salt-linked with poly(diallyldimethylammonium chloride) (PDDA) to form a three-component PDDA–Hb–KPVS complex[4] which is insoluble in aqueous solvents and functions as a cyanide ion exchanger.[5] Thus it is also interesting to study extensively the complexation of protein with polyelectrolyte in connection with the preparation of other polyelectrolyte complexes which have functions as a biomedical material and an immobilized enzyme.

In the present study, human serum albumin (HSA) was chosen as the protein component in view of the available

0024-9297/82/2215-1618$01.25/0